Published in final edited form as:
Circ Arrhythm Electrophysiol. 2013 August ; 6(4): . doi:10.1161/CIRCEP.113.000114.

A Novel Method for Determining the Phase of T-Wave Alternans: Diagnostic and Therapeutic Implications

Omid Sayadi, PhD[1], **Faisal M. Merchant, MD**[4], **Dheeraj Puppala, MD**[1], **Theofanie Mela, MD**[2], **Jagmeet P. Singh, MD, PhD**[2], **E. Kevin Heist, MD, PhD**[2], **Chris Owen, MS**[3], and **Antonis A. Armoundas, PhD**[1,5]

[1]Cardiovascular Research Center, Massachusetts General Hospital, Boston, MA

[2]Cardiology Division, Massachusetts General Hospital, Boston, MA

[3]Neurosurgery Division, Massachusetts General Hospital, Boston, MA

[4]Cardiology Division, Emory University School of Medicine, Atlanta, GA

[5]Institute for Medical Engineering and Science, Massachusetts Institute of Technology, Cambridge, MA

Abstract

Background—T-wave alternans (TWA) has been implicated in the pathogenesis of ventricular arrhythmias and sudden cardiac death (SCD). However, in order to effectively estimate and suppress TWA, the phase of TWA must be accurately determined.

Methods and Results—We developed a method that computes the beat-by-beat integral of the T-wave morphology, over time points within the T-wave with positive alternans. Then, we estimated the signed derivative of the T-wave integral sequence which allows the classification of each beat to a binary phase index. In animal studies, we found that this method was able to accurately identify the T-wave phase in artificially induced alternans ($p<0.0001$). The coherence of the phase increased consistently after acute ischemia induction in all body-surface and intracardiac leads ($p<0.0001$). Also, we developed a phase resetting detection algorithm that enhances the diagnostic utility of TWA. We further established an algorithm that employs the phase of TWA in order to deliver appropriate polarity pacing pulses (all interventions compared to baseline, $p<0.0001$ for alternans voltage; $p<0.0001$ for K_{score}), to suppress TWA. Finally, we demonstrated that using the phase of TWA we can suppress spontaneous TWA during acute ischemia; 77.6% for alternans voltage ($p<0.0001$) and 92.5% for K_{score} ($p<0.0001$).

Conclusions—We developed a method to quantify the temporal variability of the TWA phase. This method is expected to enhance the utility of TWA in predicting ventricular arrhythmias and SCD and raises the possibility of using upstream therapies to abort a ventricular tachyarrhythmia prior to its onset.

Keywords

alternans; arrhythmia (heart rhythm disorders); pacing; implantable cardioverter-defibrillator

Correspondence: Antonis A. Armoundas, PhD, Cardiovascular Research Center, Massachusetts General Hospital, 149 13th Street, Charlestown, MA 02129, Tel: 617-726-0930, Fax: 617-726-5806, aarmoundas@partners.org.

Conflict of Interest Disclosures: All others have none.

Introduction

T-wave alternans (TWA) testing has been associated with an increased risk for ventricular tachyarrhythmic events (VTE), such as ventricular tachycardia/ventricular fibrillation (VT/VF) and sudden cardiac death (SCD)[1], during *medium* and *long*-term follow-up[2, 3].

However, beyond medium- and long-term risk prediction, several lines of pre-clinical and clinical evidence suggest that the presence of heightened TWA may play a more proximal role in creating the substrate necessary for malignant ventricular arrhythmias[4–6]. Analysis of intra-cardiac electrograms from ICD leads has demonstrated a sharp increase in TWA magnitude immediately prior to spontaneous ventricular arrhythmias[7–9], without a similar upsurge in TWA prior to induced ventricular arrhythmias or preceding inappropriate ICD shocks[7]. Simultaneous measurement of TWA from body-surface and intra-cardiac electrograms by our group[10] and others[11] has shown a high degree of correlation, suggesting that these measurements are detecting the same electrical phenomenon. In aggregate, the clinical and experimental data suggest that the heart either passes through a state of heightened T-wave alternans on the way to VT/VF or heightened TWA occurs in close conjunction with developing VTE[12, 13]. In either scenario, these findings suggest that detecting significantly elevated levels of TWA may serve as an important *short*-term predictor of impending arrhythmias and also raise the possibility for a *therapeutic* role where TWA suppression therapies are delivered upstream to suppress the arrhythmogenic substrate and abort VT/VF prior to arrhythmia onset[214].

The clinical application of TWA, whether it serves a diagnostic role for medium- and long-term risk prediction or a therapeutic role for guiding short-term upstream anti-arrhythmic therapy, requires the ability to accurately estimate TWA. It has been reported that abnormal beats with altered morphology and/or timing present inherent difficulties in the estimation of alternans[15], primarily by provoking changes in TWA phase[16]. However, assessment of the alternans phase, a term which refers to the specific phase of an alternating sequence of long/short or large/small T-waves, has generally been underappreciated in clinical TWA testing. Current algorithms used to estimate TWA classify premature ventricular contractions (PVCs) and beats following transient prolongation or shortening of the cycle length as “bad” beats, but they do not estimate the phase of TWA either preceding or following such “bad” beats. However, a “bad” beat may cause phase resetting of TWA and therefore may either reduce the amplitude of alternans[15] or potentiate the amplitude of alternans[16]. In either case, PVCs may significantly hamper the TWA estimation by generating a false positive or a false negative result. Therefore, the development of methods to estimate the phase of TWA before and after a “bad” beat and consequently accounting for changes in phase, may significantly improve the performance of TWA as a diagnostic test for predicting medium- and long-term arrhythmia risk[17, 18].

Similarly, the ability to estimate the phase of TWA is also likely to have a critical impact on designing potential therapeutic strategies to suppress TWA and mitigate short-term arrhythmia risk. However, as has been demonstrated[2], lack of *a priori* knowledge of the phase of TWA (long/short or large/small T-wave) may increase the amplitude of alternans and potentiate, rather than suppress, the arrhythmogenic substrate. Therefore, developing methods to estimate the phase of alternans in real-time is likely to play an important role in designing therapies to suppress TWA.

In this study, we aim to examine the hypothesis that algorithms to estimate the phase of TWA in intracardiac and body-surface signals can improve the diagnostic and therapeutic utility of TWA.

Methods

Animal Preparation

24 male Yorkshire swine (40–45 kg) were anesthetized and acutely instrumented in the Animal Electrophysiology Laboratory of the Massachusetts General Hospital. The protocol was approved by the Hospital's Animal Care and Use Committee.

Anesthesia was induced with Telazol (4.4 mg/kg) IM and Xylazine (2.2 mg/kg) IM. Each subject was intubated and placed on a mechanical ventilator, and anesthesia was maintained with Isoflurane (1.5–5%).

Standard electrocardiographic electrodes were placed on the subject's limbs and chest; the epidermis was excised at point of contact to maximize signal quality. An arterial line was used to monitor arterial blood pressure. Percutaneous intracardiac access was achieved in the jugular veins and femoral arteries and veins using standard Seldinger techniques. Decapolar catheters were placed under fluoroscopic guidance in the (i) right ventricle (RV), the distal lead being at the RV apex, (ii) coronary sinus (CS), the distal lead being at the distal CS, (iii) left ventricle (LV), the proximal lead being at the LV apex. An inferior vena cava catheter was inserted as a reference electrode for unipolar signals.

Regional myocardial ischemia was induced in 11 subjects via balloon occlusion of the proximal left circumflex coronary artery utilizing standard percutaneous cardiac catheterization techniques[10].

Equipment and Data Collection Methods

Intracardiac and body-surface (leads II and V4) electrocardiographic signals as well as arterial blood pressure were recorded through a Prucka Cardiolab (General Electric) electrophysiology system that provided 16 high fidelity analog output signals, as previously described[10,14]. We used a previously developed signal acquisition, analysis and display system, consisting of custom software written in LabView 8.5 (National Instruments, Austin, TX) and MATLAB 7.6 (Mathworks, Natick, MA)[10].

Details of the alternans estimation algorithm[10,14] are provided in the Online Supplement. T-wave alternans estimates were obtained from two body-surface leads and 12 intracardiac unipolar leads (three in each of the RV, LV, and CS catheters).

We have employed a programmable stimulator that is capable of dynamically delivering pacing pulses on a beat-to-beat basis. Each pacing pulse is triggered upon detection of an ECG waveform (the R-wave)[14].

T-Wave Alternans Phase Estimation

The algorithm we developed to estimate the phase of TWA is presented in Figure 1A, and is described below. In order to compute a phase index (PI) that differentiates between the two phases of TWA (Figure 1B), we devised a method that is based on the integral of the T-wave. The method relies on computing the beat-by-beat integral of the T-wave morphology (Figure 1C) between the onset and offset T-wave points (as determined by the wavelet transform).

To maximize the effect of T-wave samples with significant alternans on the integral value and at the same time to account for the temporal characteristics of the TWA, we estimated the alternans voltage and K_{score}[8, 10] on a point-by-point basis throughout the T-wave, using a rolling 128-beat window that was shifted one beat at a time. Then, the integral was calculated at each time point within the T-wave with statistically significant TWA (that is points with $K_{score}>3$ and alternans voltage greater than a lead-dependant threshold[10]) and normalized to

the number of points used for the integral estimation. This improved integral provides a more accurate means of determining the phase of the alternating T-waves.

To overcome subtle changes in the beat-to-beat T-wave morphology that may affect the phase estimation, we introduce the signed derivative of the T-wave integral which allows the classification of each beat to a binary phase index that takes two different values: +1 or −1 corresponding to large/small integral values, respectively (Figure 1D).

Finally, to minimize the sensitivity of the algorithm to an arbitrary ECG reference channel, we have devised an artificial alternating reference phase index sequence (+1,−1,+1,−1,…) time series against which the phase time series of each lead is compared.

To quantitatively investigate the degree of synchronous alternation between two waveforms, the coherence of two signals (estimated phase and reference phase) has been estimated using the Welch's averaged periodogram method (for more information, please see the Online Supplement)[19].

Statistical Methods

Aggregate variables were expressed as mean±standard deviation. Box-plot representation including the median, 90-10% and 95-5% percentiles was used to demonstrate statistical properties of the estimated coherence in data sequences with/without repolarization alternans. For each channel, coherence values were compared before and after R-wave triggered pacing using the Wilcoxon signed-rank test. The phase of TWA was compared across catheters using the Kruskal-Wallis analysis of variance. Comparisons between alternans voltage and K_{score} across leads before and after R-wave triggered pacing used 2-way ANOVA. The 95% confidence intervals for sensitivity, specificity, positive predictive value, negative predictive value and accuracy were calculated based on binomial distribution. A p value of <0.05 was used to determine statistical significance. Statistical analysis was performed using MATLAB (MathWorks Inc, Natick, MA) and STATA (StataCorp LP, College Station, TX).

Results

Evaluation of the Estimation of the TWA Phase in the Normal Heart

We evaluated the ability of the algorithm to accurately estimate the phase of TWA using R-wave triggered pacing during the absolute refractory period. Pacing pulses of (i) amplitude: ±1 mA and ±5 mA, (ii) width: 30 ms and (iii) coupling to the R-wave: 10 ms were delivered during the absolute refractory period on every other beat basis from two leads (RV12) of a decapolar catheter, at the apex of the RV, to modulate ventricular repolarization and induce TWA.

To investigate the ability of our algorithm to determine the phase of the T-wave, we estimated the PI at baseline and following R-wave triggered pacing. We then evaluated the coherence at 0.5 cycles/beat between the artificial alternating reference PI sequence and the PI series for each of the leads at the body-surface and CS, LV and RV catheters, before and after R-wave triggered pacing. For each K_{score} and alternans voltage, TWA was considered positive if $K_{score}>3$ and alternans voltage was greater than the lead-specific thresholds (body-surface: 0.55 μV; CS: 1.98 μV, LV: 4.18 μV, RV: 4.235 μV)[10]. The box plot representation of the phase coherence distributions for sequences of negative and positive alternans during all 4 pacing protocols are shown in Figure 2A for body-surface and intracardiac leads. The summary statistics demonstrate that the coherence is significantly higher for positive alternans than negative alternans across all leads on the body-surface and intracardiac leads ($p<0.0001$ for all paired comparisons, n=36 for each of the body surface, CS, LV and RV leads; where n

represents the overall sample size: 9 subjects for each of the ±1 mA and ±5 mA pacing interventions).

Then, to estimate the phase coherence thresholds for body-surface and intracardiac leads, we estimated the receiver operating characteristic (ROC) curve for coherence values ranging from 0 to 1 and computed the true and false detection rates for positive and negative alternans using the coherence values, as follows: using the TWA criteria described above (for K_{score} and alternans voltage), the estimated coherence indicated a true positive or false negative outcome if it was greater or smaller than the corresponding threshold. Similarly, if alternans was negative, the coherence estimate was considered a false positive or true negative depending on whether its value was greater or smaller than the corresponding threshold.

In Figure 2B we plot the sensitivity (Sn) and specificity (Sp) for body-surface and intracardiac leads as a function of coherence threshold. The corresponding ROC curves are shown in Figure 2C. The area under the curve for body-surface leads and intracardiac CS, LV and RV catheters was: 0.99, 0.95, 0.98 and 0.99, respectively. For each lead configuration, the optimal phase coherence threshold was determined as the point that has the minimum distance to the point (Sn,1−Sp) = (1,0), which is equal to minimizing $[(1-Sn)^2 + (1-Sp)^2]^{0.5}$ (Figure 2C). The estimated thresholds for body-surface leads and CS, LV and RV leads were: 0.419, 0.376, 0.406 and 0.647, respectively. These thresholds are shown by the horizontal lines in Figure 2A. The corresponding Sn and Sp pairs at the threshold were estimated to be: (0.95,0.95), (0.89,0.89), (0.93,0.91) and (0.96,0.98) for body-surface and CS, LV and RV leads, respectively.

Evaluation of the Estimation of the TWA Phase in the Presence of Acute Ischemia

To investigate the ability to estimate the phase of spontaneous TWA, we applied our algorithm on body-surface and intracardiac (CS, LV and RV leads) electrograms recorded before (baseline) and during acute ischemia. The number of beats per subject recorded before and during coronary artery occlusion was 848±334 and 954±532, respectively (p=0.69, signed-rank=23, n=10). The mean heart rate at baseline and during coronary artery occlusion was 106.7±9.2 bpm, and 109.2±20.1 bpm, respectively (p=1, signed-rank=0, n=10).

The alternans voltage was significantly higher ($p<0.0001$ for all paired comparisons, n=80 where n represents the total number of comparisons: 40 for baseline and 40 during ischemia, 10 for each of the body surface, CS, LV, and RV leads) during coronary artery occlusion compared to baseline: 0.12±0.17 μV vs. 6.12±6.23 μV, 0.25±1.01 μV vs. 10.39±9.42 μV, 0.60 ±1.69 μV vs. 19.13±12.88 μV and 0.51±1.70 μV vs. 24.86±19.29 μV, for body-surface and CS, LV and RV leads, respectively. Similarly, the K_{score} was significantly higher ($p<0.0001$ for all paired comparisons, n=80 where n represents the total number of comparisons: 40 for baseline and 40 during ischemia, 10 for each of the body surface, CS, LV, and RV leads) during coronary artery occlusion compared to baseline: 0.87±1.61 vs. 189.72±366.96, 0.14±0.51 vs. 29.60±43.10, 0.27±0.76 vs. 68.08±126.66 and 0.15±0.48 vs. 90.44±176.76, for body-surface and CS, LV and RV leads, respectively.

In Figure 3 we summarize the compiled results (n=10) of the coherence distributions for electrograms recorded before and during acute ischemia. The coherence is significantly higher for ischemia-induced TWA than baseline across all leads on the body-surface and intracardiac leads ($p<0.0001$ for all paired comparisons, n=80 where n represents the total number of comparisons: 40 for baseline and 40 during ischemia, 10 for each of the body surface, CS, LV, and RV leads). No statistically significant difference was observed as a function of lead type, including between body-surface and any of the intracardiac catheter leads (baseline: Kruskal-Wallis test, p=0.62, n=10; post balloon occlusion: Kruskal-Wallis test, p=0.88, n=10; where n is the number of study subjects used in this comparison). These results suggest that an increase

of the TWA magnitude during acute ischemia is associated with an increase of the corresponding coherence, while as expected during baseline when TWA was deemed negative, the associated coherence values were significantly lower.

To evaluate the performance of the algorithm to estimate the phase in the presence of myocardial ischemia, we applied the previously ROC-derived phase coherence thresholds to the results reported in Figure 3 (Table 1). We observe that the accuracy of the estimation for body-surface, CS, LV and RV leads is 0.91, 0.94, 0.93 and 0.90, respectively. These results suggest that coherence thresholds estimated from artificially induced alternans can be applied to the acute ischemia model and yield highly accurate estimates of the TWA phase in both body surface and intracardiac leads.

Detection of TWA Phase Resetting

Having examined the ability of the proposed method to estimate the phase of TWA, we evaluated the use of the PI as a means to detect phase resetting (Figure 4). In order to detect potential TWA phase resetting, we estimated the cross-correlation of the estimated TWA phase with that of the reference phase index sequence, which at the point of phase resetting is expected to result to a zero-crossing and a change in the polarity of the correlation coefficient (please, see Online Supplement).

In Figures 4A–4D, we demonstrate the performance of the proposed phase resetting detection algorithm in two different study subjects in body surface electrograms recorded during myocardial infarction. The first subject shows a reduction of the alternans voltage and K_{score} caused by phase resetting from a PVC at beat numbers 628 and 831 (lead V4). The second subject shows an artificial increase of the alternans voltage and K_{score} caused by a PVC at beat number 350 (lead V4). Each of these two PVCs results in an abrupt decrease/increase in the estimated correlation of the phase of the signal with that of the reference channel, manifested by a zero-crossing of the correlation coefficient and changes in the sign of the correlation coefficient before and after the zero-crossing point.

We applied the phase-resetting detection algorithm to all 10 subjects during acute ischemia and found a total of 67 incidents of phase resetting out of 224 QRS-complex morphology changes (i.e. PVCs), yielding a 30% probability of experiencing phase-resetting when a bad beat occurs. This signifies the relatively high incidence of artificial modulation of TWA estimation, which can now be determined by the proposed phase-resetting detection algorithm.

Utility of the TWA Phase to Trigger Appropriate Electrical Therapy

After evaluating the ability of the proposed method to estimate the phase of artificially induced and spontaneously occurring TWA, we evaluated its performance as a means to guide electrical therapy aimed to suppress TWA.

Specifically, we employed R-wave triggered pacing pulses during the absolute refractory period to induce and suppress TWA from two catheter leads in the RV (induction lead: RV12; suppression lead: RV34 or RV56; pulse amplitude: +/−7 mA; pulse width: 30ms; coupling to R-wave: 30ms). In Figure 5, baseline (intervention A) corresponds to alternans induced during R-wave triggered pacing from RV12 on an every other beat basis, while subsequent interventions refer to the effect of varying the R-wave triggered stimulus polarity delivered from RV34 or RV56 with respect to the phase of alternans (induced from RV12). In interventions (B)–(E) R-wave triggered pacing from RV12 continues on an every even beat basis; however, triggered stimuli are now delivered from RV34 or RV56 on every odd beat (B and C) or every even beat (D and E) with −7 mA (B and E) or +7 mA (C and D).

In order to establish a relationship between the outcome of the R-wave triggered pacing with the pacing pulse polarity and the phase of TWA, we estimated the alternans voltage and K_{score} using the protocol described above and reported the product of: (pacing polarity)×(phase polarity). *Phase polarity* is defined as positive when the stimulus from RV34 or RV56 is triggered on beats with the opposite phase to the phase of alternans at baseline (out of phase pacing). In contrast, *phase polarity* is defined as negative when the RV34 or RV56 stimulus is triggered on beats with the same phase as the phase of alternans at baseline (in-phase pacing). The alternans voltage and K_{score} for body surface, CS, LV and RV leads for each of the above interventions is shown in Figure 5 (n=8). We observe that in-phase pacing with negative pulse polarity, as well as out of phase pacing with positive pulse polarity, results in TWA increase, while in-phase pacing with positive pulse polarity or out of phase pacing with negative pulse polarity results in a reduction of TWA (comparison between baseline and each of the interventions used to suppress alternans for each lead type: $p<0.0001$ for alternans voltage; $p<0.0001$ for K_{score} for the same paired interventions, n=8).

These results demonstrate that lack of a priori knowledge of the phase of TWA may result in an increase in the TWA amplitude (as shown in interventions C and E). Therefore, in order to effectively suppress TWA, one needs to know the phase of the estimated TWA. Based on these results, we propose that when the alternans phase and pacing pulse have opposite polarity, R-wave triggered pacing will decrease TWA.

Utility of the TWA Phase to Suppress Spontaneous TWA During Acute Ischemia

We have further evaluated the utility of the phase-dependent R-wave triggered pacing during the absolute refractory period to suppress spontaneous TWA in sinus rhythm, *in vivo*.

In Figure 6, we plot the K_{score} of a triangular intra-cardiac bipolar lead configuration CS2CS8, LV4CS2 and LV10CS2 (an optimized intra-cardiac alternans detection lead system[14]), following coronary artery balloon occlusion. In intervention A, one observes significant spontaneously occurring TWA. Upon detection of significant TWA, we estimated the phase of TWA and applied in-phase R-wave triggered pacing with positive polarity from a catheter lead in the right ventricle apex with the following parameters: amplitude: +4 mA; pulse width: 10 ms; pulse coupling: 10 ms, on every even beat (intervention B). We observe that R-wave triggered pacing results to a significant reduction of spontaneous TWA during acute ischemia (77.59% average reduction across the 3 leads of the alternans voltage compared to baseline, $p<0.0001$; 92.55% average reduction across the 3 leads of the K_{score} compared to baseline, $p<0.0001$). In intervention c, RV12 triggered pacing is discontinued, leading to increase of the alternans voltage and K_{score} (68.62% average increase across the 3 leads of the alternans voltage compared to TWA suppression, $p<0.0001$; 87.06% average increase across the 3 leads of the K_{score}, compared to TWA suppression, $p<0.0001$).

Incidentally, pacing on an every beat basis does not decrease the level of alternans (data not shown). This finding is further supported by our recent observation[14] that pacing during the absolute refractory period on every beat basis, induces a consistent, lead-dependent modulation on ventricular repolarization. These data provide an important proof of concept that the phase of TWA is a critical parameter of TWA that can be estimated in real-time and be used to suppress spontaneously occurring TWA.

Discussion

In light of extensive pre-clinical[12, 13, 20–22, 23] and clinical data[8, 9, 11, 24] demonstrating an association between heightened TWA and the onset of malignant arrhythmias including VT/VF, the accurate detection and potential modulation of TWA may hold promise as a method to predict and preempt lethal heart rhythm disturbances. We have previously shown that a

premature beat may alter the phase of alternans with significant implications on the estimation of TWA and its predictive utility[15]. The main aim of this study was to establish a robust method to quantify the temporal variability of TWA phase, and use it to enhance the medium- and long-term SCD risk prediction of TWA as well as to guide short-term electrical therapy to suppress TWA.

This study is the first to provide a comprehensive and systematic approach to determine the phase of TWA in body-surface and intracardiac leads. Specifically, *first* we have shown that the method we have developed to estimate the phase of TWA is robust and sensitive to subtle changes of the T-wave morphology. *Second*, use of an artificial alternating reference phase index sequence allows the real time estimation of the temporal dynamics of the TWA phase. *Third*, during acute ischemia the phase-derived coherence can discriminate between negative and positive TWA levels, and provide highly accurate estimates of the TWA phase. *Fourth*, the phase-derived coherence can be used to determine phase-induced variability of TWA that results to significant improvement in the TWA estimation. *Fifth*, the phase of TWA and the polarity of a pacing pulse are sufficient to define a pacing strategy to suppress TWA in-vivo. *Sixth*, we have been able to demonstrate that the TWA phase can be used to suppress spontaneously occurring TWA following acute myocardial infarction, *in-vivo*.

Our results may have important clinical applications for diagnostic and therapeutic procedures that are based on TWA estimation. From a diagnostic point of view, microvolt TWA testing has emerged as an important predictor of SCD during medium- and long-term follow-up[25, 26]. However, although the negative predictive value of TWA testing has generally been good, the positive predictive value has been much less robust[27]. Our data suggest that methods to improve the positive and negative predictive value of TWA testing may significantly improve its predictive utility. It has previously been shown that the presence of PVCs or other "bad" beats (with altered morphology and/or timing) may have a profound detrimental effect on TWA testing by either underestimating[15] or overestimating[16] the level of TWA. Our study extends these prior findings by demonstrating in a swine model of acute coronary ischemia that PVCs frequently lead to modulation of TWA. The presence of PVCs is very common during clinical TWA testing and the presence of frequent PVCs is the most common reason for indeterminate test results[10]. Additionally, the likelihood of indeterminacy increases with progressively more impaired left ventricular systolic function[26], suggesting that patients at highest risk of SCD may be particularly susceptible to false-positive or false-negative TWA results due to PVC induced phase resetting. The algorithm developed and validated in this study may provide a robust method for detecting scenarios where phase reversals are likely to lead to false-positive or false-negative TWA estimates and thus may significantly improve the sensitivity, positive and negative predictive value of TWA testing.

Furthermore, studies in humans in which TWA was measured during ventricular pacing have demonstrated that the presence of alternans phase reversal after PVCs carries important prognostic information and predicts a significantly lower arrhythmia-free survival when compared to patients without post-PVC phase reversal[28]. However, extension of these findings has been limited by the lack of a validated method to measure the alternans phase in an efficient manner. Our data suggest that in addition to improving positive and negative predictive value, incorporating information about phase reversal into clinical TWA testing algorithms may independently improve the utility of non-invasive TWA testing for medium- and long-term SCD risk prediction.

From a therapeutic perspective, several lines of pre-clinical and clinical evidence suggest that the presence of heightened TWA may play a causative or permissive role in creating an arrhythmogenic substrate and setting the stage for impending ventricular arrhythmias[29]. It has been suggested that appropriately timed pacing therapy, potentially delivered from an

implantable device (e.g. ICD), may be capable of suppressing the amplitude of TWA and potentially pre-empting the onset of VT/VF[142]. In order for such upstream therapies to be viable, several conditions must be met. First, TWA must be detectable from an implantable device in real-time with a high degree of sensitivity and fidelity. In this regard, we have developed and tested a novel intra-cardiac lead configuration which is capable of highly sensitive spatial and temporal alternans detection[10]. Second, once a state of heightened TWA is detected, device-delivered therapy must be administered with the goal of rapidly suppressing the alternans magnitude and quelling the arrhythmogenic substrate. We have recently demonstrated that R-wave triggered pacing pulses delivered during the absolute refractory period are capable of suppressing TWA[142]. However, the outcome of R-wave triggered pacing therapy is critically dependent on the alternans phase and if pacing therapy does not consider the TWA phase, the amplitude of TWA may be potentiated rather than suppressed. Therefore, being able to measure the TWA phase in real-time and then deliver customized therapy is a critical step in being able to reproducibly suppress TWA. In this study, we have demonstrated the importance of phase and pacing pulse polarity in determining the response to pacing therapy. Specifically, in-phase pacing with positive polarity pulses or out of phase pacing with negative polarity pulses provides a consistent suppression effect on TWA. It is likely that TWA suppression helps reduce repolarization gradients and thus reduce arrhythmia susceptibility. The important relationships established in this paper between phase polarity and response to R-wave triggered therapy are likely to become a crucial step in designing future studies that specifically assess the effect of alternans suppression algorithms on arrhythmia inducibility with the aim of validating the concept of upstream therapy. However, it should be noted that acute ischemia induced alternans and SCD may have a different physiology than chronic ischemic related alternans and SCD.

In conclusion, our findings support the idea that the temporal variability of the phase of TWA can be effectively estimated by analysis of subtle changes of the T-wave amplitude that occur on a beat-to-beat basis. The algorithm presented in this study aims to enhance both the diagnostic and therapeutic clinical utility of TWA estimation.

Supplementary Material

Refer to Web version on PubMed Central for supplementary material.

Acknowledgments

Funding Sources: The work was supported by a Scientist Development Grant (#0635127N) and a Founders Affiliate Post-doctoral Fellowship (#12POST9310001) from the American Heart Association, and by NIH grant 1R21AG035128. This work was also supported by a Fellowship and a Science Award from the Center for Integration of Medicine and Innovative Technology (CIMIT), the Deane Institute for Integrative Research in Atrial Fibrillation and Stroke and the Cardiovascular Research Society. This work was conducted with support from Harvard Catalyst, The Harvard Clinical and Translational Science Center (National Center for Research Resources and the National Center for Advancing Translational Sciences, National Institutes of Health Award 8UL1TR000170-05 and financial contributions from Harvard University and its affiliated academic health care centers). The content is solely the responsibility of the authors and does not necessarily represent the official views of Harvard Catalyst, Harvard University and its affiliated academic health care centers, or the National Institutes of Health.

Theofanie Mela, MD (Honoraria: Medtronic < $10K, Biotronik < $10K, St Jude < $10K); Jagmeet P Singh MD, PhD (Research Grants: St. Jude Medical, Medtronic Inc., Boston Scientific Corp., Biotronik; Advisory Board / Steering Committee/Consultant: Boston Scientific Corp., Biotronik, St. Jude Medical, Medtronic, CardioInsight Inc, Thoratec Inc, Biosense Webster, Honoraria / Speaker Fees: Medtronic Inc., Biotronik, Guidant Corp., St. Jude Medical, Sorin Group; E. Kevin Heist MD, PhD (Honoraria (modest amount): Biotronik, Boston Scientific, Medtronic, Sorin, St Jude Medical; Research grants (modest amount): Biotronik, Boston Scientific, St Jude Medical; Consultant (modest amount): Boston Scientific, Sanofi, Sorin, St Jude Medical).

References

1. Bloomfield DM, Hohnloser SH, Cohen RJ. Interpretation and classification of microvolt T wave alternans tests. J Cardiovasc Electrophysiol. 2002; 13:502–512. [PubMed: 12030535]
2. Merchant FM, Armoundas AA. Role of substrate and triggers in the genesis of cardiac alternans, from the myocyte to the whole heart: implications for therapy. Circulation. 2012; 125:539–549. [PubMed: 22271847]
3. Merchant FM, Sayadi O, Moazzami K, Puppala D, Armoundas AA. T-wave Alternans as an Arrhythmic Risk Stratifier: State of the Art. Curr Cardiol Rep. 2013 (In Press).
4. Narayan SM, Bayer JD, Lalani G, Trayanova NA. Action potential dynamics explain arrhythmic vulnerability in human heart failure: a clinical and modeling study implicating abnormal calcium handling. J Am Coll Cardiol. 2008; 52:1782–1792. [PubMed: 19022157]
5. Ng GA, Brack KE, Patel VH, Coote JH. Autonomic modulation of electrical restitution, alternans and ventricular fibrillation initiation in the isolated heart. Cardiovasc Res. 2007; 73:750–760. [PubMed: 17217937]
6. Weiss JN, Karma A, Shiferaw Y, Chen PS, Garfinkel A, Qu Z. From pulsus to pulseless: the saga of cardiac alternans. Circ Res. 2006; 98:1244–1253. [PubMed: 16728670]
7. Kim JW, Pak HN, Park JH, Nam GB, Kim SK, Lee HS, Jang JK, Choi JI, Kim YH. Defibrillator electrogram T wave alternans as a predictor of spontaneous ventricular tachyarrhythmias in defibrillator recipients. Circ J. 2009; 73:55–62. [PubMed: 19039191]
8. Armoundas AA, Albert CM, Cohen RJ, Mela T. Utility of implantable cardioverter defibrillator electrograms to estimate repolarization alternans preceding a tachyarrhythmic event. J Cardiovasc Electrophysiol. 2004; 15:594–597. [PubMed: 15149432]
9. Swerdlow CD, Zhou X, Voroshilovsky O, Abeyratne A, Gillberg J. High amplitude T-wave alternans precedes spontaneous ventricular tachycardia or fibrillation in ICD electrograms. Heart Rhythm. 2008; 5:670–676. [PubMed: 18452868]
10. Weiss EH, Merchant FM, d'Avila A, Foley L, Reddy VY, Singh JP, Mela T, Ruskin JN, Armoundas AA. A novel lead configuration for optimal spatio-temporal detection of intracardiac repolarization alternans. Circ Arrhythm Electrophysiol. 2011; 4:407–417. [PubMed: 21430127]
11. Paz O, Zhou X, Gillberg J, Tseng HJ, Gang E, Swerdlow C. Detection of T-wave alternans using an implantable cardioverter-defibrillator. Heart Rhythm. 2006; 3:791–797. [PubMed: 16818208]
12. Pastore JM, Girouard SD, Laurita KR, Akar FG, Rosenbaum DS. Mechanism linking T-wave alternans to the genesis of cardiac fibrillation. Circulation. 1999; 99:1385–1394. [PubMed: 10077525]
13. Pastore JM, Rosenbaum DS. Role of structural barriers in the mechanism of alternans-induced reentry. Circ Res. 2000; 87:1157–1163. [PubMed: 11110773]
14. Armoundas AA, Weiss EH, Sayadi O, Laferriere S, Sajja N, Mela T, Singh JP, Barrett CD, Kevin Heist E, Merchant FM. A novel pacing method to suppress repolarization alternans in vivo: implications for arrhythmia prevention. Heart Rhythm. 2013; 10:564–572. [PubMed: 23274372]
15. Armoundas AA, Mela T, Merchant FM. On the estimation of T-wave alternans using the spectral fast fourier transform method. Heart Rhythm. 2012; 9:449–456. [PubMed: 22001706]
16. Hashimoto H, Suzuki K, Nakashima M. Effects of the ventricular premature beat on the alternation of the repolarization phase in ischemic myocardium during acute coronary occlusion in dogs. J Electrocardiol. 1984; 17:229–238. [PubMed: 6207256]
17. Chow T, Kereiakes DJ, Onufer J, Woelfel A, Gursoy S, Peterson BJ, Brown ML, Pu W, Benditt DG. Does microvolt T-wave alternans testing predict ventricular tachyarrhythmias in patients with ischemic cardiomyopathy and prophylactic defibrillators? The MASTER (Microvolt T Wave Alternans Testing for Risk Stratification of Post-Myocardial Infarction Patients) trial. J Am Coll Cardiol. 2008; 52:1607–1615. [PubMed: 18992649]
18. Cantillon DJ, Stein KM, Markowitz SM, Mittal S, Shah BK, Morin DP, Zacks ES, Janik M, Ageno S, Mauer AC, Lerman BB, Iwai S. Predictive value of microvolt T-wave alternans in patients with left ventricular dysfunction. J Am Coll Cardiol. 2007; 50:166–173. [PubMed: 17616302]
19. Bendat, JS.; Piersol, AG. Engineering applications of correlation and spectral analysis. 1st ed.. New York: John Wiley and Sons, Inc; 1980.

20. Baker LC, London B, Choi BR, Koren G, Salama G. Enhanced dispersion of repolarization and refractoriness in transgenic mouse hearts promotes reentrant ventricular tachycardia. Circ Res. 2000; 86:396–407. [PubMed: 10700444]
21. Choi BR, Salama G. Simultaneous maps of optical action potentials and calcium transients in guinea-pig hearts: mechanisms underlying concordant alternans. J Physiol. 2000; 529(Pt 1):171–188. [PubMed: 11080260]
22. Qu Z, Garfinkel A, Chen PS, Weiss JN. Mechanisms of discordant alternans and induction of reentry in simulated cardiac tissue. Circulation. 2000; 102:1664–1670. [PubMed: 11015345]
23. Shimizu W, Antzelevitch C. Cellular and ionic basis for T-wave alternans under long-QT conditions. Circulation. 1999; 99(11):1499–1507. [PubMed: 10086976]
24. Christini DJ, Stein KM, Hao SC, Markowitz SM, Mittal S, Slotwiner DJ, Iwai S, Das MK, Lerman BB. Endocardial detection of repolarization alternans. IEEE Trans Biomed Eng. 2003; 50:855–862. [PubMed: 12848353]
25. Armoundas AA, Hohnloser SH, Ikeda T, Cohen RJ. Can microvolt T-wave alternans testing reduce unnecessary defibrillator implantation? Nat Clin Pract Cardiovasc Med. 2005; 2:522–528. [PubMed: 16186850]
26. Armoundas AA, Tomaselli GF, Esperer HD. Pathophysiological basis and clinical application of T-wave alternans. J Am Coll Cardiol. 2002; 40:207–217. [PubMed: 12106921]
27. Gehi AK, Stein RH, Metz LD, Gomes JA. Microvolt T-wave alternans for the risk stratification of ventricular tachyarrhythmic events: a meta-analysis. J Am Coll Cardiol. 2005; 46:75–82. [PubMed: 15992639]
28. Narayan SM, Smith JM, Schechtman KB, Lindsay BD, Cain ME. T-wave alternans phase following ventricular extrasystoles predicts arrhythmia-free survival. Heart Rhythm. 2005; 2:234–241. [PubMed: 15851310]
29. Merchant FM, Ikeda T, Pedretti RF, Salerno-Uriarte JA, Chow T, Chan PS, Bartone C, Hohnloser SH, Cohen RJ, Armoundas AA. Clinical utility of microvolt T-wave alternans testing in identifying patients at high or low risk of sudden cardiac death. Heart Rhythm. 2012; 9:1256–1264. e1252. [PubMed: 22406384]

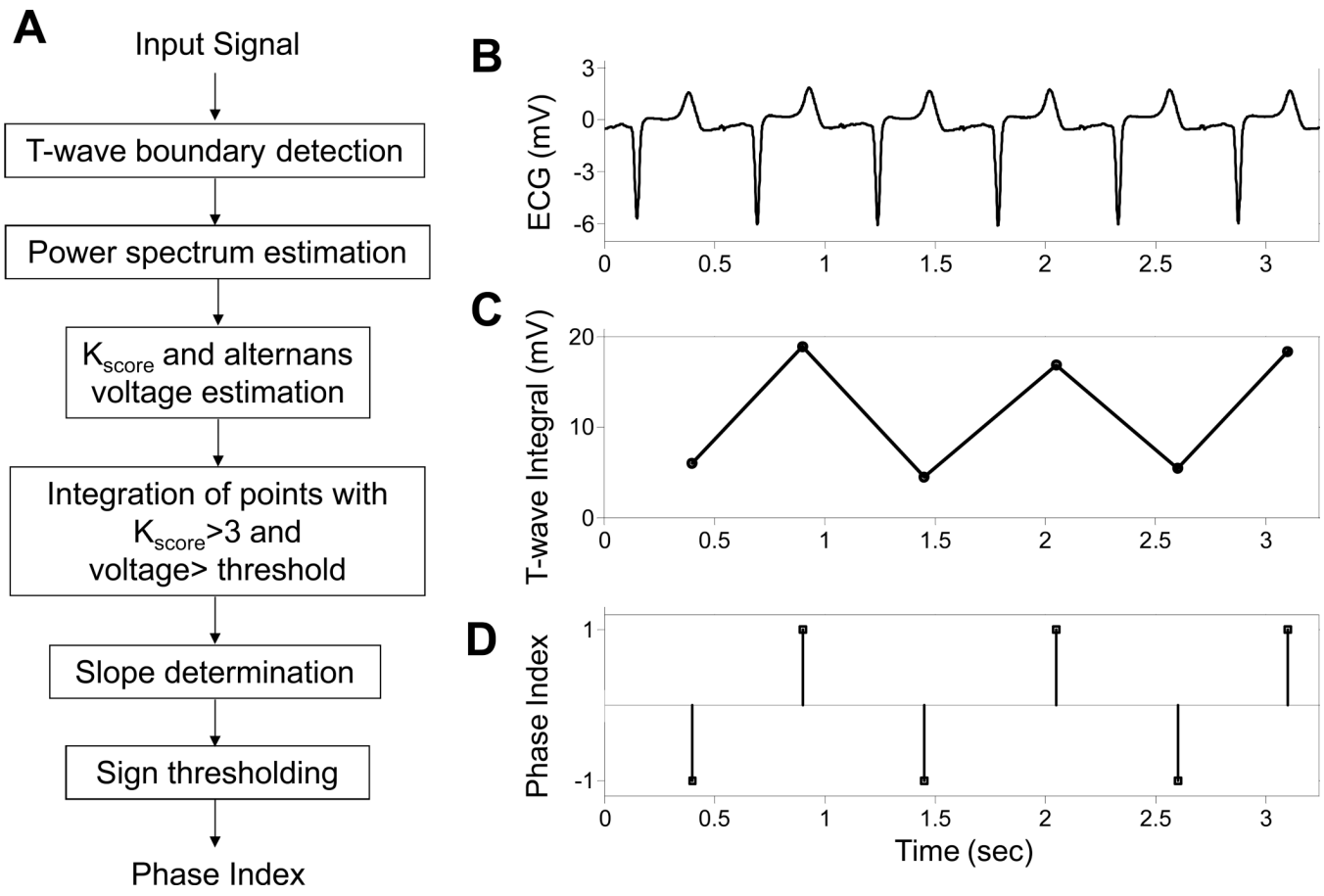

Figure 1.
Algorithm for estimating the phase of repolarization alternans (A). Example of an intracardiac left ventricular lead (LV1U) electrogram (B) used to estimate the integral of the T-wave (C) and the binary phase index (D).

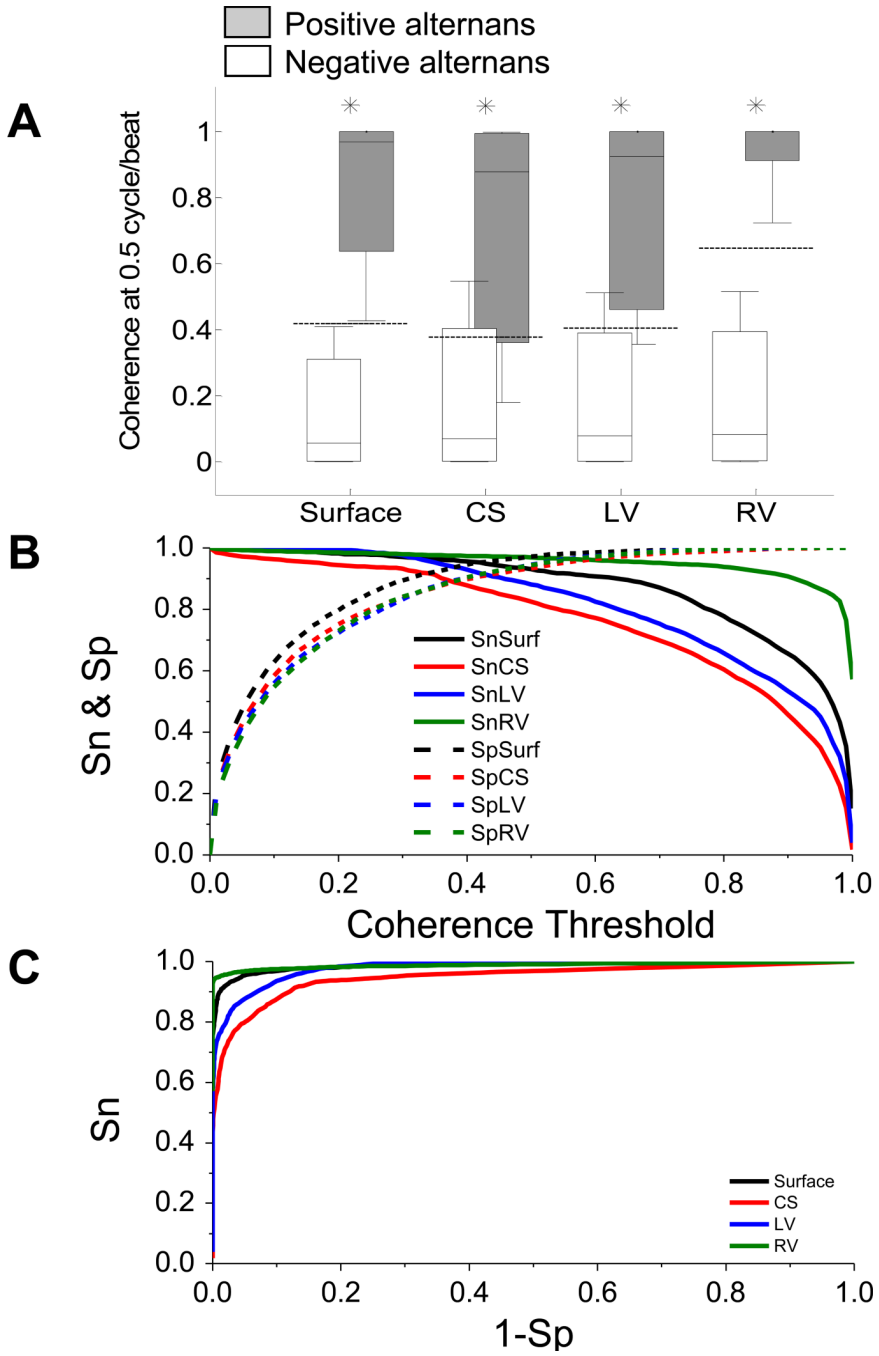

Figure 2.

Statistical coherence analysis of 4 pacing protocols (amplitude: ±1/±5 mA, pulse width: 30 ms, coupling: 10 ms) in the normal heart (n=9) for negative and positive alternans sequences. (A) Box-plot representation of the estimated coherence value at 0.5 cycle/beat for negative alternans (white boxes) and positive alternans (gray boxes) during baseline and following R-wave triggered pacing for body-surface and CS, LV and RV leads. For each set of body-surface leads and intracardiac leads, the median (horizontal solid line), 90-10% percentiles (box) and 95-5% percentiles (error bars) are shown. The dashed lines indicate the lead-dependent coherence threshold determined using the corresponding ROC curve. (n=36 for each of the

body surface, CS, LV and RV leads; where n represents the overall sample size: 9 subjects for each of the ±1 mA and ±5 mA pacing interventions) (B) Sensitivity (Sn) and specificity (Sp) for body-surface and intracardiac leads as a function of their respected coherence threshold. (C) ROC curves for body-surface leads and intracardiac leads determined by changing the coherence threshold from 0 to 1 in steps of 0.001. For each lead, statistically significant comparisons (negative alternans vs. positive alternans) are marked by an asterisk.

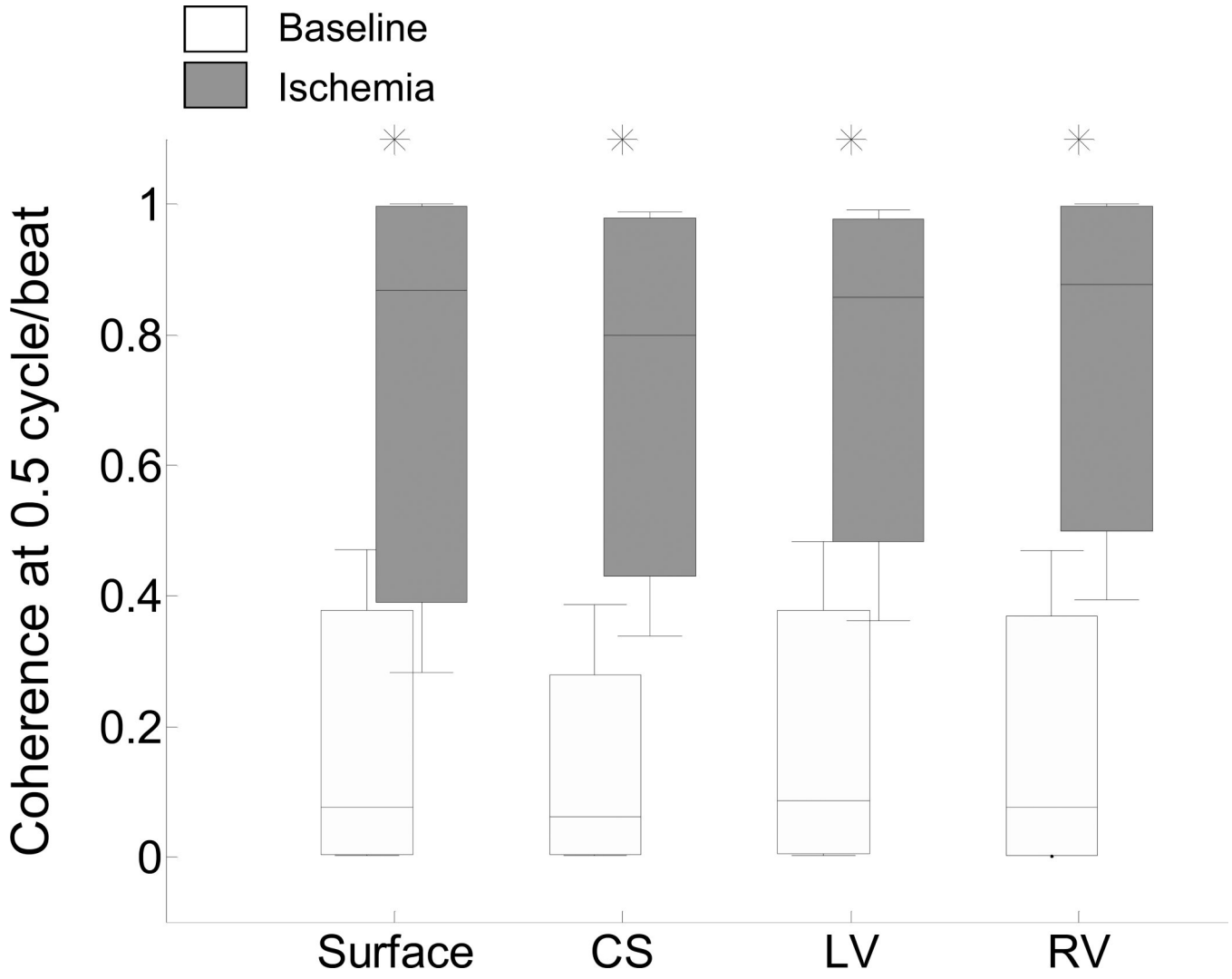

Figure 3.

Statistical coherence analysis before (white boxes) and during (gray boxes) circumflex coronary artery balloon occlusion for body-surface and RV, CS, LV and RV leads. For each group of body-surface and intracardiac leads, the median (horizontal solid line), 90-10% percentiles (box) and 95-5% percentiles (error bars) are shown. Coherence increased during acute ischemia in all leads ($p<0.0001$, $n=80$ where n represents the total number of comparisons: 40 for baseline and 40 during ischemia, 10 subjects for each of the body surface, CS, LV, and RV leads). No statistically significant difference was observed between any lead type (baseline: Kruskal-Wallis test, $p=0.62$, $n=10$; post balloon occlusion: Kruskal-Wallis test, $p=0.88$, $n=10$; where n is the number of study subjects used in this comparison). For each lead, statistically significant comparisons (baseline vs. ischemia) are marked by an asterisk.

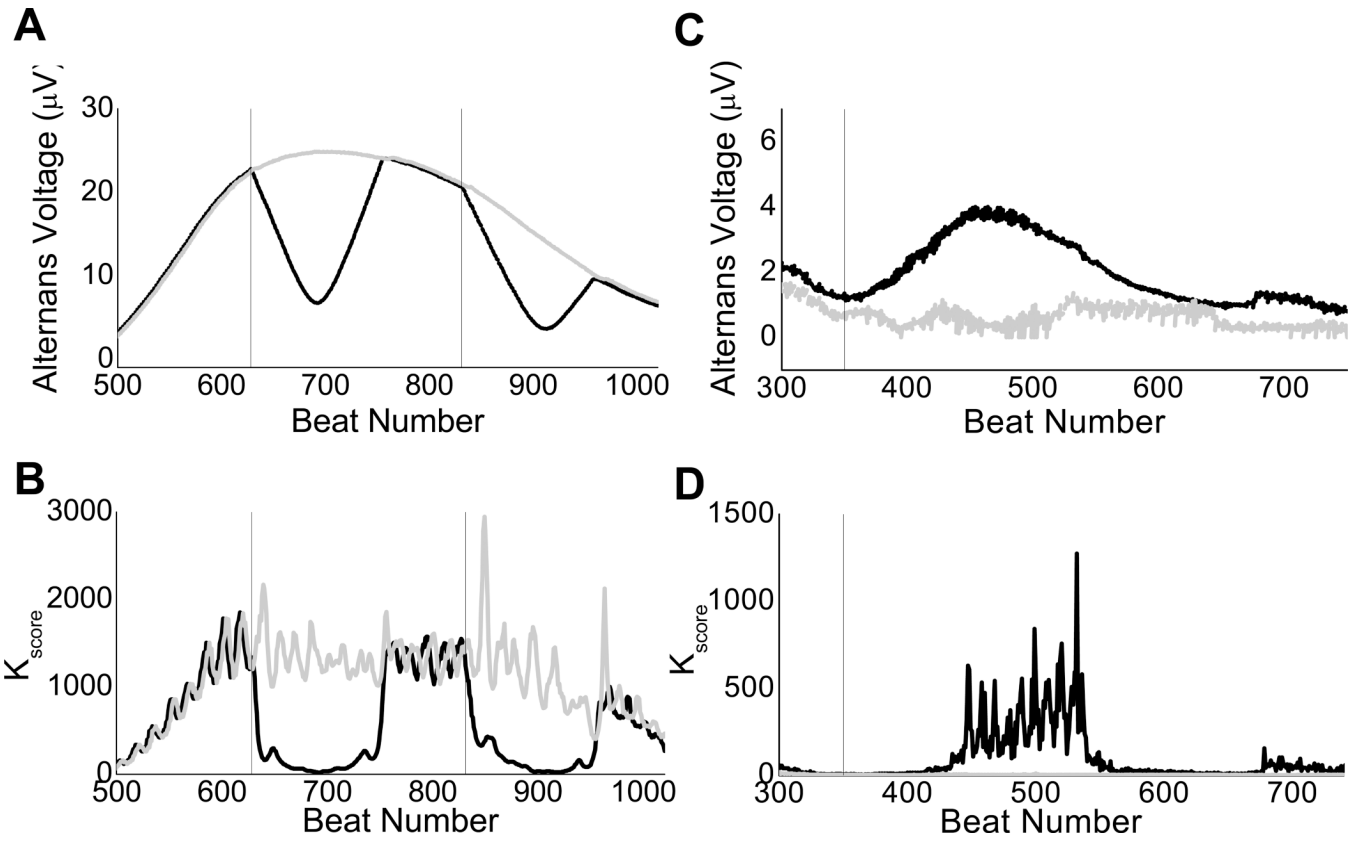

Figure 4.

Use of phase estimation to detect phase resetting. Effect of phase resetting on the alternans voltage (A and C) and K_{score} (B and D) estimation on a body-surface lead in two different study subjects (subject 1: panel A and B, subject 2: panel C and D). Artificial decrease (A) or increase (C) of the alternans voltage with concomitant K_{score} artificial decrease (B) or increase (D), are in each case associated with the presence of phase resetting caused by a premature ventricular contraction. Detection and removal of phase resetting (in black) results to the corrected alternans voltage and K_{score} estimation (in gray). Dashed vertical lines indicate the index of the PVC.

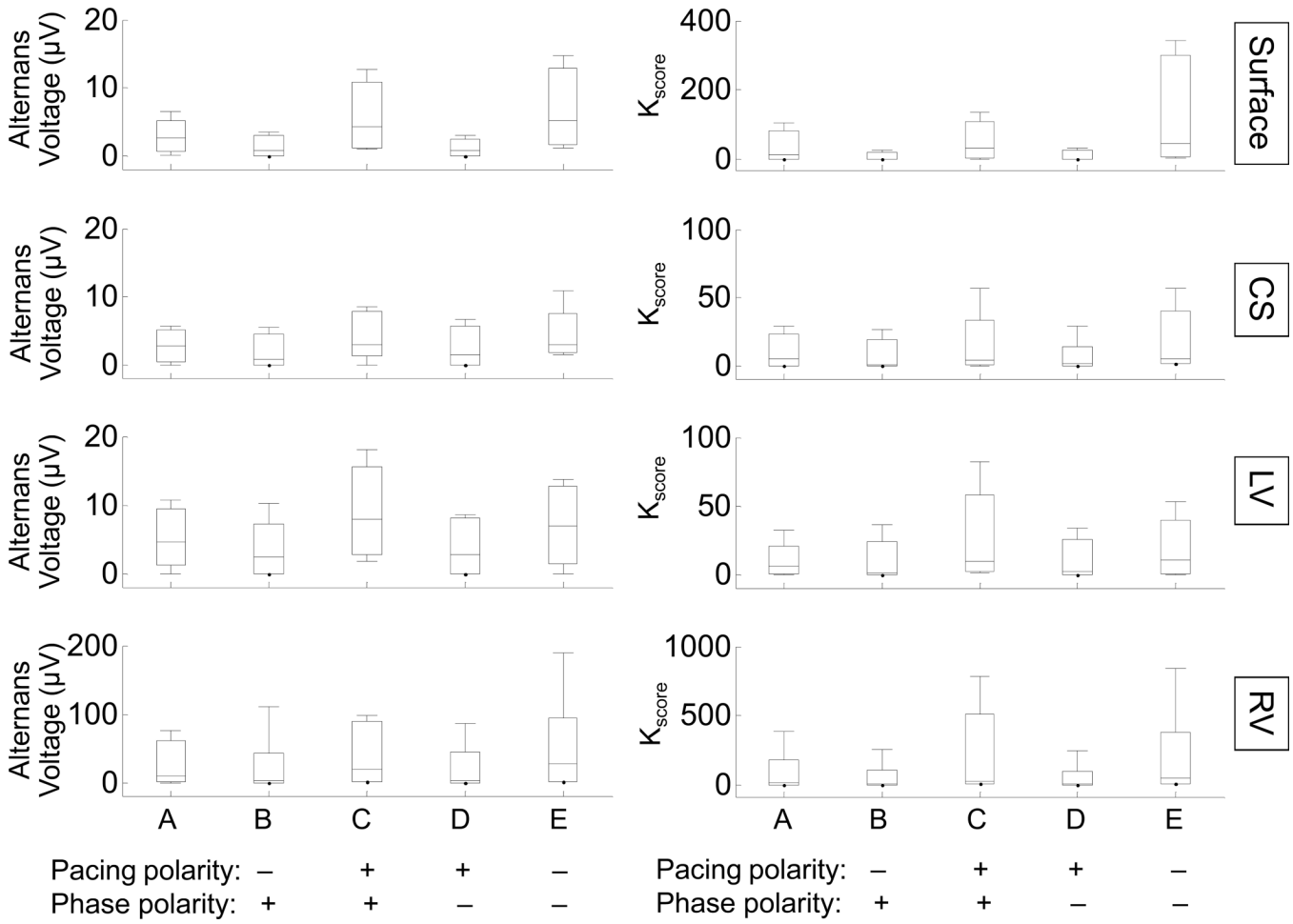

Figure 5.

Algorithm to suppress T-wave alternans using the phase of TWA and the pacing pulse polarity. The distribution of alternans voltage (left column) and K_{score} (right column) is shown for alternans baseline (through R-wave triggered pacing on alternate beats from lead RV12) and following phase perturbation (through R-wave triggered pacing from RV34 or RV56 leads) for body surface, CS, LV and RV leads (n=8). The (pacing polarity)×(phase polarity) for the interventions following the alternans baseline is shown on horizontal axis. For each intervention, the median (horizontal solid line), 90-10% percentiles (box) and 95-5% percentiles (error bars) are shown. Both alternans voltage and K_{score} increased for interventions with positive (pacing polarity)×(phase polarity). In contrast, both alternans voltage and K_{score} decreased for interventions with negative (pacing polarity)×(phase polarity).

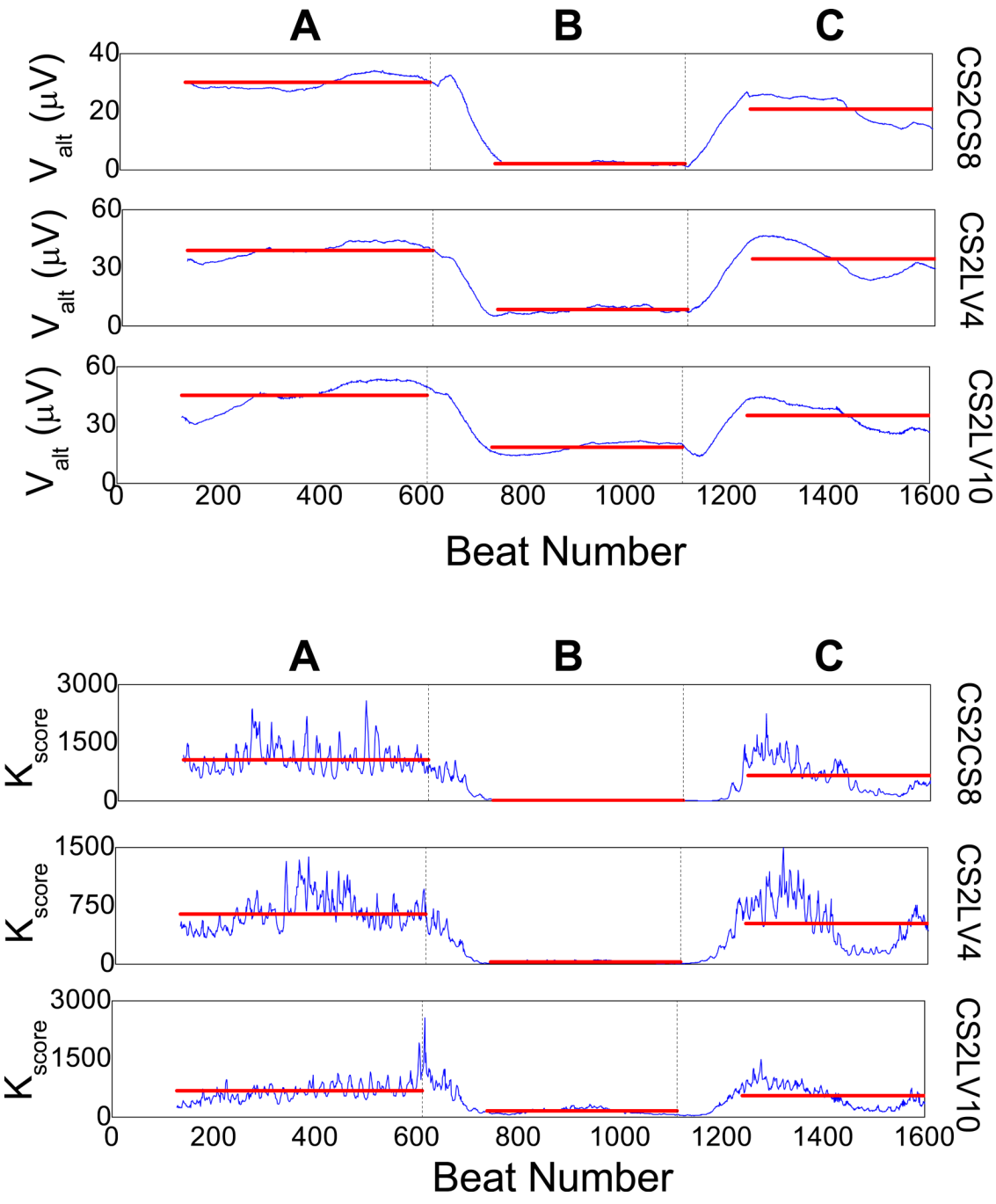

Figure 6.

Utility of the T-wave alternans (TWA) phase to suppress spontaneously occurring alternans in sinus rhythm during acute myocardial ischemia. Alternans voltage and K_{score} are plotted for the intra-cardiac lead configuration CS2CS8, CS2LV4 and CS2LV10. In-phase suppression pacing intervention is delivered from the right ventricle apex (RV12; amplitude: +4 mA, width: 10 msec, coupling to R-wave: 10 msec). **A**: spontaneously occurring alternans is visible at baseline, **B**: R-wave triggered pacing is delivered from RV12 on every even beat with a positive polarity pulse, which results to significant reduction of TWA (77.59% reduction of the alternans voltage compared to baseline, $p<0.0001$; 92.55% reduction of the K_{score} compared

to baseline, $p<0.0001$), **C**: R-wave triggered pacing is discontinued and both alternans voltage and K_{score} increase to the baseline level during sinus rhythm. Transitions **A** to **C** occur correspondingly at times marked by solid vertical black lines, while the colored horizontal lines during each intervention indicate the mean value of the alternans voltage and K_{score} during that intervention.

Table 1

Performance evaluation of phase estimation during acute ischemia. For each of the body-surface, CS, LV and RV leads the ROC-derived thresholds, determined in artificially induced TWA in control swine, have been applied to the coherence estimation results reported in Figure 3. The 95% confidence intervals are shown in parentheses.

	Lead			
	Surface	**CS**	**LV**	**RV**
Sn	0.89 (0.88–0.90)	0.93 (0.92–0.94)	0.94 (0.93–0.94)	0.80 (0.79–0.81)
Sp	0.93 (0.92–0.94)	0.95 (0.94–0.95)	0.92 (0.91–0.92)	1.00 (1.00-1.00)
PV+	0.93 (0.92–0.93)	0.95 (0.94–0.95)	0.92 (0.91–0.93)	1.00 (1.00-1.00)
PV−	0.90 (0.89–0.90)	0.93 (0.92–0.94)	0.93 (0.93–0.94)	0.83 (0.83–0.84)
Accuracy	0.91 (0.90–0.92)	0.94 (0.94-0.94)	0.93 (0.92–0.94)	0.90 (0.90-0.90)

(Sn: Sensitivity; Sp: Specificity; PV+: Positive predictive value; PV−: Negative predictive value).